AIMS Energy, 13(4): 922–937.
DOI: 10.3934/energy.2025034
Received: 19 April 2025
Revised: 16 July 2025
Accepted: 29 July 2025
Published: 12 August 2025

https://www.aimspress.com/journal/energy

Research article

Performance studies on PVT assisted solar drying of municipal solid waste for enhancement of heat generation during combustion

Mohammed A. Alanazi* and Zakariya Kaneesamkandi

Department of Mechanical Engineering, College of Engineering, King Saud University (KSU), Riyadh 12372, Saudi Arabia

* **Correspondance:** Email: malanazif@ksu.edu.sa; Tel: +966114670859.

Abstract: Incineration technologies for municipal solid waste have undergone many developments in terms of control equipment for efficient emissions and advanced combustion technologies such as fluidized bed combustion systems. Excessive moisture in the waste of organic materials has resulted in storage problems, pest and bacterial infections, odor, and difficulties in pre-processing before combustion. Size reduction of waste components is important for efficient combustion; however, moisture is a detriment to this process. The importance of drying the organic materials within waste was discovered and led to the creation of several drying methods, both using conventional and non-conventional energy sources. In this study, a totally grid independent photovoltaic thermal dryer with unity solar fraction was installed for municipal solid waste drying and the performance of functional components, namely, the photovoltaic system, the solar heater, and the drying chamber, were evaluated for arid desert climatic conditions for year-round performance. The photovoltaic system was used to energize the fan for the dryer air supply and panel cooling. The effect of air cooling on the photovoltaic panel power was evaluated. The solar air heater parameters, namely the heat removal factor and the overall loss coefficient were experimentally determined. Waste samples collected in the cities of Riyadh and Dammam under two climate conditions were tested to determine the drying rates and optimum drying bed thicknesses. The actual drying rates and its impact on the energy produced during waste combustion were determined. The results and economic analysis indicate that the overall gains achieved after implementing this drying method increase the economic performance of waste to energy systems.

Keywords: heating value enhancement; municipal solid waste; photovoltaic thermal; photovoltaic thermal collector; solar drying

Abbreviations: MSW: Municipal Solid Waste; PVT: Photovoltaic thermal; PV: Photovoltaic; HHV: Higher Heating Value; LHV: Lower Heating Value

1. Introduction

As of 2018, more than 1 billion tons of waste is produced worldwide and is expected to rise to 2.2 billion by the end of 2025 [1]. About 70% of the municipal solid waste (MSW) is landfilled, 19% is recycled, and 11% is converted to energy [2]. Waste-to-energy supply chains help to mitigate both disposal problems and the demand for energy [3]. The incineration of waste is an effective means to reduce the MSW volume to much smaller volumes and to recover energy at the same time. There is approximately a 60% reduction in weight and up to a 90% reduction in volume [4]. Combustion and emissions control measures have been developed by new and efficient designs and have been successfully implemented to make sure that the emissions meet the necessary standards [5]. MSW incineration is usually done by either a mass burn grate firing method or by fluidized bed combustion. Grate firing is done by two methods: sloping grate or vibrating grate. Fluidized bed combustion can be a bubbling bed technology or a circulating fluidized bed technology.

The storage of MSW, which has a moisture content of more than 40%, has become one of the operating challenges for waste storage and incinerators. Organic wastes such as vegetable wastes have a high moisture content (88–94%) and cause major environmental problems at municipal dumpsites [6]. Moisture plays a key role in the decomposition of MSW, and a 20% to 30% moisture content aids this process [7]. The effects of moisture on the anaerobic digestion of MSW were studied at different moisture dosing rates, and a significant increase in the digestion rate was reported [8]. Excessive moisture can result in leachates, especially if the waste is dumped on loose soil. The formation of odors is another undesirable consequence of excessive moisture in the waste. Moreover, the grindability of the waste is also affected by the presence of high moisture [9]. Since the waste is reduced in size in grinding mills, the energy consumption for the grinding process increases with an increase in the moisture content. Moisture affects the sustainability of the combustion process of the municipal waste by reducing its calorific value due to the heat absorbed for the evaporation of the water in it. The annual average calorific value of wet MSW must not be below 7 MJ/kg in order to maintain a viable incineration process [10].

The effect of the MSW fuel size on the combustion process in a fixed bed was analyzed, and it was found that sizes greater than 50 mm resulted in a decrease in the combustion temperature and a decrease in the emission of greenhouse gases [11]. A system to reduce moisture by thermal drying of MSW was proposed to reduce pollutants and to improve the overall efficiency of a combustion system using the waste heat recovery from the flue gas. The calculations showed that the lower heating value of the MSW increased to 9,000 kJ/kg at drying temperatures of 533 K for a duration of 10 minutes. The incineration temperatures were found to be acceptable [12].

A reduction in the moisture content in MSW can increase the heat available through combustion, which can be used for heat production or electricity generation through direct usage or usage in the form of refuse derived fuel pellets [13–15].

Different methods have been adopted to dry MSW. Bio-drying involves the use of heat generated during the aerobic conversion of organic material to dry the fresh waste material. The greenhouse type of bio-dryer used with solar energy required a temperature from 40 to 70 ℃ and sufficient aeration inside the reactor [16]. Solar greenhouse dryers used to dry tomatoes produced an increase in the air temperature between 20 to 40 ℃ [17]. Bio-stabilization involves proper pretreatment of the waste and then subjecting it to biodegradation, but the process time is much higher [18]. Solar drying involves heating air using solar energy and using circulation and operating temperatures from 50 to 60 ℃ [19]. Thermal drying was found to achieve 100% dry waste, but the associated fuel cost to produce the hot air at temperatures ranged from 107 to 167 ℃ with a short drying time from 160 to 260 minutes [20]. The drying temperatures required for different methods of drying MSW were found to be 59 ± 37 ℃ for solar drying, 58 ± 11 ℃ for bio-stabilization, 115 ± 40 ℃ for thermal drying, and 55 ± 15 ℃ for bio-drying. Thermal drying, although an expensive option, provided the shortest drying time [21].

Lower initial and operating costs have favored the use of solar drying as the most practical and economical method for MSW. Applications of this method for pre-processing the waste before combustion or gasification reduce the overall cost of energy produced either as electrical power or process heat. Essentially, the drying process has two forms of input for efficient operation: the high temperature of the drying medium, which is air, and the continuous air change rates to transport the evaporated moisture from the material. The air temperature can be increased using solar collectors, which has undergone several improvements over the past several years. Technological developments in solar air heating for drying applications have been widely discussed, including natural and forced convection [22]. The energy required to supply air to the product that is dried can be supplied from both conventional and non-conventional sources. The concept of photovoltaic thermal (PVT) solar collectors has developed recently with both power and heat sources. The performance of PVT collectors with different configurations have been studied, both experimentally and numerically, for various applications that require heat and electricity [23].

The present experimental work was performed to determine the drying performance using a PVT-driven hot air supply system coupled with a solar air heater. The dual advantage of PVT systems, which can provide hot air and electrical fan power, which are equally important for drying, has been utilized for MSW drying. These systems were investigated to dry a wide range of materials, including agricultural products (e.g., fruits, vegetables, and herbs), food, and other materials. In this study, the concept of after heating the hot air produced from the PVT system was introduced. This ensures higher air temperatures at the drying bed. The material for drying was MSW as procured from the source. The solar panel performance and drying efficiencies were determined using an engineering equations solver. The overall efficiency of this grid independent drying mechanism was determined for a particular operating condition, and the obtained results were used to estimate the annual performance. The methodology section includes the description of the experimental set up, followed by details of the analytical equations used in the calculations. The panel performance equation, the thermal performance tests on the direct solar heating, and the drying performance are explained. The results section gives the solar PV temperature and performance, the thermal performance of the PV panel, and the secondary heating zone drying results for two different climate zones.

2. Methodology

The model solar PVT dryer consists of four sections: the PV panel section, a provision for air cooling on its bottom surface, the solar air heater, and the dryer. The air circulation is maintained by the fan, which is energized by the PV panel itself. A polycrystalline PV panel is used, which is inclined at an angle equal to the latitude of the location facing south, as per the procedures established in [24]. The air flow maintained by the fan is directed to the PV panel bottom surface. The PV panel gets cooled by this air, which then moves to the solar air heater section. In the solar air heater section, the absorber plate is covered with a single layer glass plate, and air flows between the glass plate and the absorber plate. Then, the hot air from the solar air heater passes through the fan and goes to the dryer section, where a bed of MSW is spread over a perforated sheet. The solar air heater has a length of 2 m and a width of 0.5 m. The schematic layout and a picture of the experimental system is given in Figure 1.

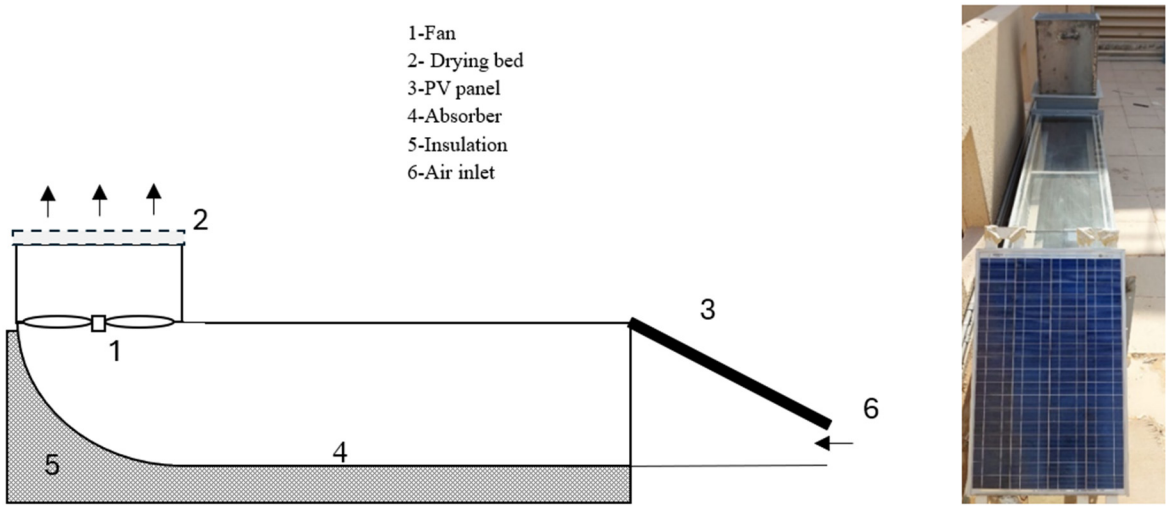

Figure 1. The schematic layout and the picture of the experimental system.

2.1. Functions and specifications of the system components

The PV panel has an area of 0.8 m × 0.5 m and is tilted to the horizontal at an angle of 25°. The air passage that leads to the solar air heater is arranged such that the air gets in contact with the bottom surface of the panel to cool the panel. Figure 1 shows the construction of the panel with the cooling duct.

The power output of the PV panel is determined based on the electrical efficiency of the panel using the following equation [25]:

$$P_o = \eta_{el} \times I_t \times A \quad (1)$$

where P_o is the electrical power output of the panel, W,
η_{el} is the electrical efficiency of the panel from Eq 2,
A is the panel area, m^2, and
I_t is the solar radiation incident on the tilted plane of the collector, W/m^2.

The theoretical electrical efficiency η_{el} is a function of the cell temperature [9] and is using the following equation:

$$\eta_{el} = \eta_{ref} \times [1 - \beta_c \times (T_c - T_{ref})], \quad (2)$$

where η_{ref} is the nominal efficiency of the panel at a standard temperature of 298 K,
T_{ref} is the reference temperature which is 298 K,
T_c is the cell temperature (K), and
β_c is the cells temperature coefficient, which indicates a drop in efficiency with the temperature. The temperature coefficient used in this panel is (–0.4)% /° C.

The solar radiation intensity is measured with a pyranometer connected to a data acquisition system with an uncertainty of ±2%, and the panel temperature is measured with a K type thermocouple with an uncertainty less than ±0.25 ℃. The efficiency of the PV cell is calculated from the measured temperature and, based on this efficiency, the power output of the panel is determined.

2.2. Solar panel F_R and U_L determination

The performance characteristics of the solar air heater are the heat removal factor, F_R, and the collector's overall loss coefficient, U_L. These are determined by the "ΔT over I", in which the Hottel-Whillier-Bliss (HWB) equation is divided by the heat collected by the solar collector using the following equation [9]:

$$\eta_C = F_R \times (\tau\alpha) - \left[\frac{F_R U_L}{I_t} \times \left(T_{fi} - T_a\right)\right]. \quad (3)$$

The variation of efficiency with the value of $[(T_{fi}-T_a)/I_t]$ gives the values of F_R and U_L by fitting the straight line and graphically identifying the slope and the y-intercept. In the above equation, T_{fi} and T_a represent the air temperatures at the inlet of the collector, and I_t represents the intensity of solar radiation. The temperature measurements are using K type thermocouples with an uncertainty less than ±0.25 ℃, and the solar radiation intensity is measured using a pyranometer with an uncertainty of ±2%.

2.3. Rate of heat production in municipal solid waste fired combustion systems

Heat produced by the combustion systems depends on the fuel composition and the combustion efficiency. The higher heating value (HHV) was calculated using the Dulong formula and decimal fractions of the individual elements carbon (C), hydrogen (H), sulfur (S), and oxygen (O) present in the waste sample using the following example [26]:

$$HHV = 0.3383 \times C + 1.443 \times H - 0.1804 \times O + 0.0942 \times S. \quad (4)$$

Online monitoring of the fuel moisture content demonstrated an increased combustion temperature and efficiency alongside a decrease in carbon monoxide emissions and fine particulate matter [27]. The HHV of a fuel is the total heat available in the fuel and the lower heating value (LHV) is the net heat available after condensation of the moisture in the flue gas [28]. The heat release rate (HRR) is the heat required to operate a power plant boiler using a solid fuel firing system and depends on the power generation rate by combustion (P_E), the boiler efficiency (η_B), and the generator

efficiency (η_G) (Eq 5). Performance tests on the boilers that used the MSW as fuel indicated a boiler efficiency of 60% and a generator efficiency of 90%. The flue gas temperature reduced when the moisture content increased in the fuel [29].

$$HRR = \frac{P_E}{\eta_B \times \eta_G} \tag{5}$$

An estimate of the LHV or the net heating value (NHV) is obtained from the measured HHV by subtracting the heat of vaporization of water in the products as follows [29]:

$$LHV = HHV \times (1 - M) - 2.447M, \tag{6}$$

where LHV is the gross (or lower) heating value in MJ/kg, and M is the weight of moisture in 1 kg of fuel. The constant 2.447 is the latent heat of vaporization of water in MJ/kg at 25 ℃. A more accurate estimate of the net heating value can be obtained by including the heat released by the combustion of the hydrogen content of the biomass. Equation 2 gives the variation of the heat produced by the combustion system ring at different moisture contents [30]. The minimum sustainable heat required depends on the capacity of the combustion system. Usually, the capacity of the combustion system depends on the quantity of waste produced in the collection area.

2.4. Drying of MSW

The drying rate or the final moisture content of the dried product depends on the airflow rate, the drying time, and the drying temperature. The temperature attained by the air that enters the drier (T_O) from the solar collector determines the drying temperature and is given by the following Eq 7 [31]:

$$T_O = T_I + \frac{q_u}{\dot{m} \times C_{Pa}}, \tag{7}$$

where T_I is the air inlet temperature, and T_a is the ambient temperature. The drying efficiency (η_d) of the solar drying process is defined as the ratio of energy involved in removing the moisture in the dried material to the energy supplied to the dryer during the drying period (Eq 7). The energy gain is the latent heat of vaporization (h_{fg}) for the mass of moisture removed (m_e), and the energy input is the energy used for drying in the form of hot air from the solar collector during the period (t) of 36 hours (Eq 8). T_o is the average hourly air temperature at the collector outlet, T_a is the ambient temperature, $\dot{m}_t$ is average hourly air mass flow rate, and C_{pa} is the specific heat of air. Note that drying happens during the drying time (t), even without the solar radiation input if there is a difference in the partial vapor pressure of the dried material and that of the air [31].

$$\eta_d = \frac{m_e h_{fg}}{\sum_{t-0}^{36} [\dot{m}_t C_{pa} (T_o - T_a) \times t \times 3600]} \tag{8}$$

2.5. Solar fraction

The solar fraction (φ) is defined as the ratio of the actual thermal energy utilized for drying and the total energy that falls on the collector (Eq 9). W is the weight of the moisture evaporated during

the average sunshine (I_T)hour t. λ_S is the latent heat of evaporation at the saturation temperature of moisture at the partial pressure which corresponds to the ambient temperature [32].

$$\varphi = \frac{W * \lambda_S}{\sum_0^t I_t} \tag{9}$$

3. Results and discussion

An experimental study about MSW drying using waste collected from households using a grid energy independent drying system and solar energy was performed. The results of the PVT system performance, the solar thermal collector performance, and the dryer performance are given below. Figure 2 shows the panel temperature with and without cooling, and Figure 3 shows the panel power output with and without cooling. A comparison was performed to endure similar conditions of solar radiation, wind speeds, and sky clearness on two consecutive days. The panel temperatures were measured using K type thermocouples, and the power output was measured using a power analyzer with total uncertainty of 0.0082 W.

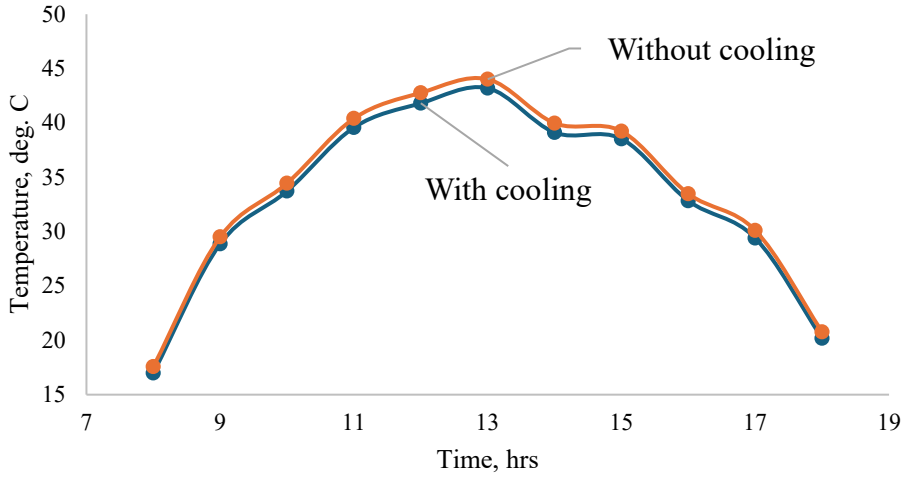

Figure 2. Panel temperature with and without cooling.

The maximum value of the power output was recorded as 43.2 W in the case of the cooling effect, and was found to be 41.8 without cooling measured under similar conditions of solar radiation, clearness of sky, and wind velocity. The gain in power output was higher during the peak solar radiation period. The results agreed with the calculated values from Eqs 1 and 2. The "ΔT over I" method was used to determine the heat removal factor (F_R) and the overall loss coefficient (U_L) of the solar air heating system as per the procedure given in Section 2. The measurements of the air temperature at the inlet to the air heater, the outlet of the air heater, and the ambient temperature were recorded using a thermocouple and a data acquisition system. The uncertainties in the thermocouples were 0.004 ℃. The air mass flow rate was determined using the average air velocity, the cross-sectional flow area, and the density of air calculated at the average temperature. Figure 4 shows the graph that was used to determine the F_R and U_L, and the results are given below.

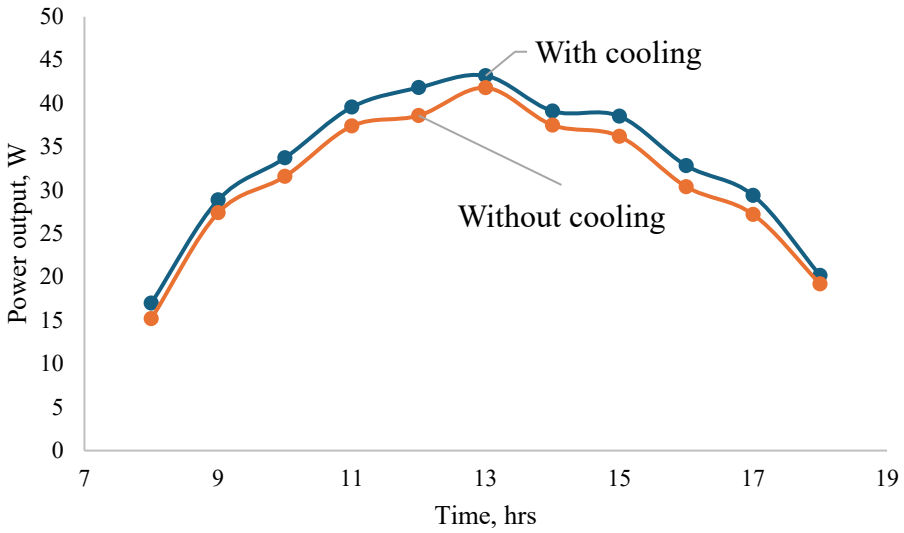

Figure 3. Panel power output with and without cooling.

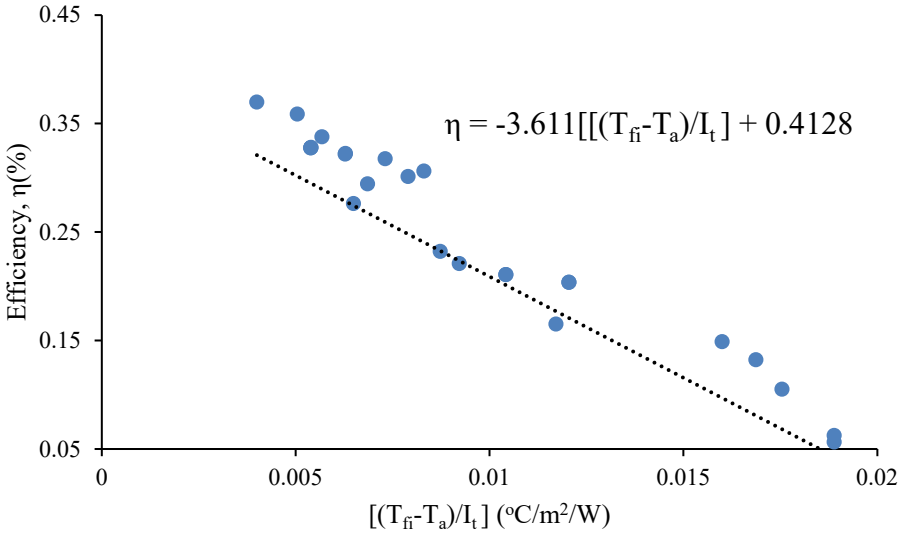

Figure 4. Solar air heater performance in terms $[(T_{fi}-T_a)/I_t]$ and collector efficiency.

The y-intercept and the slopes were obtained from the graph to determine the performance parameters. The transmissivity absorptivity coefficient used in the calculations was 0.85 for solar thermal collectors with a single normal glass and blackened steel absorber surfaces [33].

$$F_R\tau\alpha = 0.4128$$

$$F_R = 0.485$$

$$U_l F_R = 3.611$$

$$U_l = 7.43 \text{ W/m}^2\text{ K}$$

The values of F_R and U_L are in agreement with published values in the literature for solar air heaters with single glazing and flow over the absorber surface.

3.1. Moisture analysis results for samples collected from different locations and seasons

Saudi Arabia is in the hot desert climatic region, and is classified as Bwh per the Koppen climate classification [34]. MSW samples were collected from the two urban regions Riyadh and Dammam, and the moisture analysis of the organic matter in the samples were conducted as per American Society for Testing and Materials (ASTM) standards. Table 1 shows the percentage of different constituents found in the waste for the two regions. The components of the waste sample were identified based the elements in the waste, which were determined using the proximate analysis values of individual items such as plastic, paper, and so on [35].

Table 1. Percentage of components in MSW and their ultimate analysis.

Riyadh						
Component	% by weight	C	H	N	S	O
Paper	28.5	12.37	1.68	0.11	0.06	14.31
Plastic	5.2	3.74	0.48	0.04	0.02	0.92
Glass	4.6	0.00	0.00	0.00	0.00	0.00
Wood	8.0	3.73	0.47	0.11	0.02	3.67
Textiles	6.4	3.42	0.42	0.18	0.03	2.35
Organics	37.0	18.69	2.63	0.78	0.07	14.84
Others	10.3	4.31	0.65	0.14	0.03	5.18
	Total	**46.25**	**6.33**	**1.37**	**0.22**	**41.27**
Dammam						
Component	% by weight	C	H	N	S	O
Paper	16.03	6.96	0.95	0.06	0.03	8.05
Plastic	5.8	4.17	0.53	0.05	0.02	1.03
Glass	6.86	0.00	0.00	0.00	0.00	0.00
Wood	9.63	4.49	0.57	0.13	0.02	4.42
Textiles	5.77	3.09	0.38	0.16	0.02	2.12
Organics	37.0	18.69	2.63	0.78	0.07	14.84
Others	18.91	7.90	1.19	0.26	0.06	9.51
	Total	**45.29**	**6.25**	**1.45**	**0.22**	**39.96**

3.2. Determination of optimum drying bed depth

The optimum bed depth experimentally determined by repeating the drying process at different depths (h). The drying process was performed for a total of 36 hours starting from 8 am to 8 pm the following day. During this time, the active sunshine hours were from 8 am to 6 pm, for a total of 20 hours. The remaining 12 hours were the non-sunshine hours, during which drying took place at a low rate.

Figure 5 shows a decrease in the weight of the samples taken with three different bed heights of 2, 4, and 6 cm using the pH sample. The weight was taken every four hours, and the difference between the initial and final weight gives the quantity of moisture evaporated.

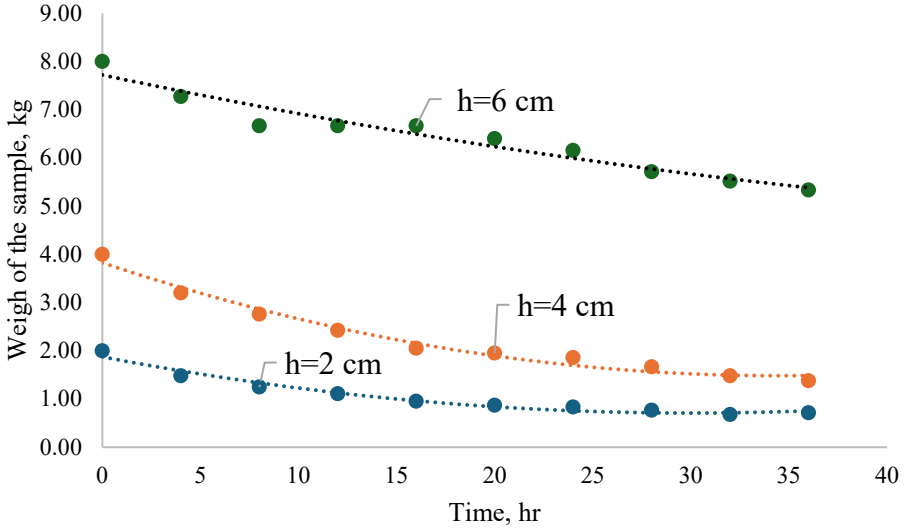

Figure 5. Decrease in weight with time for different bed heights.

The difference in weights between the beginning and end of the drying process or the water evaporated were found to be 1.29, 2.6, and 2.47 kg corresponding to the 2, 4, and 6 cm bed heights. Thus, the 4 cm bed height was taken as the optimum bed height for subsequent drying experiments.

Figures 6 and 7 show drying curves of the hot and cold weather conditions for the three samples collected from Riyadh, Jeddah, and Dammam, which are the three major urban regions in Saudi Arabia. Samples labeled Rh and Dh represent samples collected during hot season from Riyadh and Dammam, respectively. Samples labeled Rc and Dc represent samples collected from Riyadh and Dammam during the cold season, respectively.

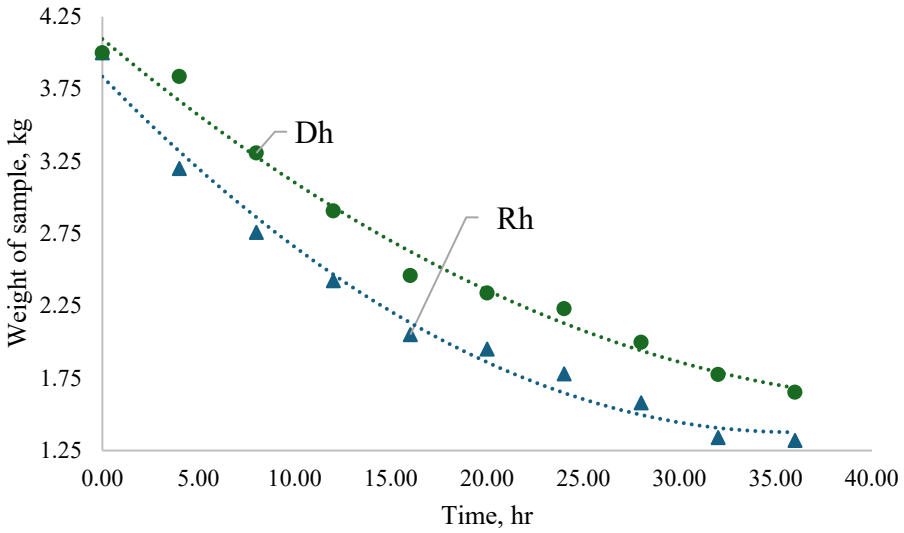

Figure 6. Decrease in the weight with time during hot climate.

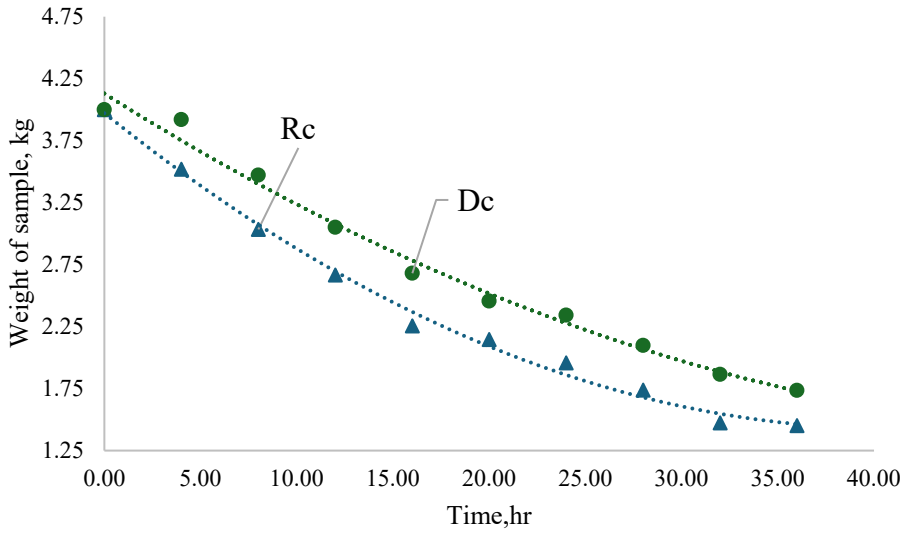

Figure 7. Decrease in weight with time during cold climate.

The drying process was recorded in the form of the weight of the sample taken with time. The total weight loss represents the quantity of water removed from the waste. The final moisture content can be calculated from this weight loss. The final moisture content in the hot season for Riyadh and Dammam waste after drying resulted in significant increase for their lower heating values. Table 2 shows the results of the analysis before and after drying for the hot weather season (May to October) and cold season (November to April), which are given separately for nonrecycling and recycling scenarios.

Table 2. Drying parameters and results of MSW heating value before and after drying for nonrecycling scenario.

	Hot season		Cold season	
	Riyadh	Dammam	Riyadh	Dammam
Average air relative humidity (%)	15	42	20	46
Average drying temperature, ℃	54	51	42	44
MSW moisture content (Before drying)	80	82	86	87
MSW moisture content (After drying)	39	57	61	67
Moisture evaporated (kg)	2.68	2.32	2.56	2.42
Thermal efficiency of drying (%)	20.62	26.78	26.52	23.20
Non recycling scenario				
LHV before drying (kJ/kg)	11916	11268	11987	11050
LHV after drying (kJ/kg)	36348	26921	36823	33944
Recycling scenario				
LHV before drying (kJ/kg)	3600	5760	4080	4828
LHV after drying (kJ/kg)	14379	17696	12536	14833

From the tables, it is observed that there is an increased amount of moisture removal during the hot season compared to the cold season. Additionally, the moisture removal for samples in Riyadh was relatively higher. This can be attributed to the atmospheric humidity, which plays an important role in the drying rate. The heat content can be calculated using Eq 5 from the results of the HHV obtained from waste components to data given in Table 1. The heat content available in the dried form of municipal waste from Riyadh and Dammam are 36,348 and 26,921 kJ/kg, respectively, for the hot season when all the constituents of the waste such as plastics, wood, rubber, paper, and organics are considered in the non-recycling scenario. When materials such as wood, paper, and plastic are recycled and only the organics are used, then the total heat contents are 14,379 and 17,696 kJ/kg, respectively, during the hot seasons for the two cities [36]. As expected, the drying is less during the cold season due to the lower drying temperature. Drying produces a significant improvement in the LHV or the NHV. The above results indicate a considerable improvement in the power generation rate after drying as per the heat release rate (Eq 5).

3.3 Drying efficiency

The efficiency of the drying process depends on various factors such as the drying temperature, the air velocity across the drying bed, the humidity of the drying air, and the nature of the material being dried. The drying process has three stages: the rising rate stage, the constant rate stage, and the falling rate stage. The constant rate and the falling rate take more time since these processes involve the movement of moisture from inside the material to the surface through the pores. The higher temperature reduces the vapor pressure around the material and aids increased drying. The higher velocity flow across the bed aids in the speedy removal of moisture from the bed. In the above experiment, the intensity of solar radiation, which changes throughout the day, determines the drying efficiency, which can be determined using Eq 8; the drying efficiency was found to be in the range of 20 to 26% for the four cases. Experiments on similar flow configurations in solar driers produced similar results of 27.5% [37,38]. The results show higher efficiency values when compared to that of solar cabinet driers used to dry other products [39]. Cabinet type solar driers were found to have an efficiency in the range of 18–20%. Drying tests conducted on the MSW using a solar greenhouse dryer produced an efficiency value of 17.01% [40]. Hence, the results from this study are encouraging and needs further testing on a larger scale.

4. Conclusions

In this study, experimental studies on a solar drying system with a PV panel powered air circulation were conducted to dry MSW. The purpose of drying was to enhance the energy recovery from the waste and to prevent waste infestation and odor. The performance characteristics of the solar thermal collector, namely the heat removal factor and the overall loss coefficient, were determined using the "ΔT over I" method, and were 0.485 and 7.43 W/m^2.K, respectively. The solar PV panel showed an efficiency improvement due to air cooling, which resulted in a higher power output of 1.4 W. The drying bed was tested for moisture reduction with 2, 4, and 6 cm thickness, and a 4 cm drying bed was identified as the optimum bed thickness. Drying tests were done with waste samples collected from two urban regions under hot and cold conditions. The period between May to October was used as the hot period, and the period between November and April was used as the cold period. The results of the

drying performance indicated significant enhancements in the heating values of the MSW by 2.5 to 3 times due to a reduced moisture content. The obtained drying efficiency was agreeable with the published data. The installation of dryers operating on solar energy helps to improve the power production in MSW fired power plants at no additional operating cost. This study is limited to tests on batch loading of the product and several challenges associated with a continuous large-scale operation need to be overcome. Future work on the continuous operation of the solar drying system for MSW is required to integrate this method in commercial incineration or gasification installations.

Use of AI tools declaration

It is declared that we didn't use AI tools.

Acknowledgments

Ongoing Research Funding Program, (ORF-2025-775), King Saud University, Riyadh, Saudi Arabia.

Conflict of interest

The authors declare no conflicts of interest.

Author's contributions

Mohammed A. Alanazi (M.A.A) worked for the measuring components in this experimental study and Zakariya Kaneesamkandi (Z.K) conducted the experimental work. The planning and preparation for the experimental work was equally contributed by M.A.A and Z.K. The preparation of the paper was done by M.A.A and Z.K and the calculations and final check was done by M.A.A and Z.K.

References

1. Palacio JCE, Santos J, Renó M, et al. (2019) Municipal solid waste management and energy recovery. In *Energy Conversion Current Technologies Future Trends,* IntechOpen. http://dx.doi.org/10.5772/intechopen.79235
2. Nowling U (2016) Waste to energy: An opportunity too good to waste, or a waste of time? Available from: http://www.powermag.com/waste-energy-opportunity-good-waste-waste-time/?pagenum=1.
3. Trindade AB, Palacio JCE, González AM, et al. (2018) Advanced exergy analysis and environmental assesment of the steam cycle of an incineration system of municipal solid waste with energy recovery. *Energy Convers Manage* 157: 195–214. https://doi.org/10.1016/j.enconman.2017.11.083
4. National Waste Policy Action Plan. Available from: https://www.dcceew.gov.au/environment/protection/waste/publications/national-waste-policy-action-plan.

5. Holmes T, Baker B, Shoemaker L (2016) Materials for service in municipal waste-& biomass-fired power generation...a review of recent experience. In *Association for Materials Protection and Performance*, 1–15. https://doi.org/10.5006/C2016-07493
6. Varma VS, Kalamdhad AS (2014) Effects of leachate during vegetable waste composting using rotary drum composter. *Environ Eng Res* 4: 67–73. https://doi.org/10.4491/eer.2014.19.1.067
7. Krause MJ, Eades W, Detwiler N, et al. (2023) Assessing moisture contributions from precipitation, waste, and leachate for active municipal solid waste landfills. *J Environ Manage* 344: 118–443. https://doi.org/10.1016/j.jenvman.2023.118443
8. Karimi S, Christopher AB (2021) The influence of moisture enhancement on solid waste biodegradation. *Waste Manage* 123: 131–141. https://doi.org/10.1016/j.wasman.2021.01.022
9. Jaya ST, Neal AY, Joshua JK (2021) Pilot-scale grinding and briquetting studies on variable moisture content municipal solid waste bales—Impact on physical properties, chemical composition, and calorific value. *Waste Manage* 125: 316–327. https://doi.org/10.1016/j.wasman.2021.02.013
10. Komilis D, Kissas K, Symeonidis A (2014) Effect of organic matter and moisture on the calorific value of solid wastes: An update of the Tanner diagram. *Waste Manage* 34: 249–255. https://doi.org/10.1016/j.wasman.2013.09.023
11. Sun R, Ismail TM, Ren XH, et al. (2016) Influence of simulated MSW sizes on the combustion process in a fixed bed: CFD and experimental approaches. *Waste Manage* 49: 272–286. https://doi.org/10.1016/j.wasman.2015.12.019
12. Zhou X, Zhou P, Zhao XQ, et al. (2021) Applicability of municipal solid waste incineration (MSWI) system integrated with pre-drying or torrefaction for flue gas waste heat recovery. *Energy* 224: 120157. https://doi.org/10.1016/j.energy.2021.120157
13. Rada EC, Ragazzi M, Panaitescu V (2015) Energy from waste: The role of bio-drying. *UPB Sci Bull Ser C: Electr Eng* 67: 69–72. Available from: https://www.researchgate.net/publication/235771548.
14. Huiliñir C, Pérez J (2017) A new model of batch biodrying of sewage sludge, Part 2: Model calibration and validation. *Drying Technol* 35: 666–679. https://doi.org/10.1080/07373937.2016.1206124
15. Tom AP, Pawels R, Haridas A (2016) Bio drying process: A sustainable technology for treatment of municipal solid waste with high moisture content. *Waste Manage* 49: 64–72. https://doi.org/10.1016/j.wasman.2016.01.004
16. Negoi RM, Ragazzi M, Apostol T (2009) Bio drying of Romanian municipal solid waste: An analysis of its viability. *UPB Sci Bull Ser C* 71: 193–204.
17. Ahmed EL-SHEIKHA, Mohamed RD, Rashad H, et al. (2024) Study the thermal performance of drying tomatoes using a solar energy system. *Inmateh Agri Eng* 23: 13–29. https://doi.org/10.35633/inmateh-73-01
18. Sugni M, Calcaterra E, Adani F (2005). Biostabilization and biodrying of municipal solid waste by inverting air-flow. *Bioresour Technol* 96: 1331–1337. https://doi.org/10.1016/j.biortech.2004.11.016
19. Kumar M, Sansaniwal SK, Khatak P (2016) Progress in solar dryers for drying various commodities. *Renewable Sustainable Energy Rev* 55: 346–360. https://doi.org/10.1016/j.rser.2015.10.158

20. Bukhmirov VV, Kolibaba OB, Gabitov RN (2015) Experimental research of solid waste drying in the process of thermal processing. *IOP Conf Ser: Mater Sci Eng* 93: 1–5. http://dx.doi.org/10.1051/matecconf/20152301057
21. Tun MM, Juchelková D (2018) Drying methods for municipal solid waste quality improvement in the developed and developing countries: A review. *Environ Eng Res* 24: 529–542. https://doi.org/10.4491/eer.2018.327
22. Lingayat A, Zachariah R, Modi A (2022) Current status and prospect of integrating solar air heating systems for drying in various sectors and industries. *Sustainable Energy Technol Assess* 52: 1022–74. https://doi.org/10.1016/j.seta.2022.102274
23. Gupta A, Biswas A, Das B (2022) Development and testing of novel photovoltaic-thermal collector-based solar dryer for green tea drying application. *Sol Energy* 231: 1072–1091. https://doi.org/10.1016/j.solener.2021.12.030
24. Gharakhani Siraki A, Pillay P (2012) Study of optimum tilt angles for solar panels in different latitudes for urban applications. *Sol Energy* 86: 1920–1928. https://doi.org/10.1016/j.solener.2012.02.030
25. Triyanto A, Abdul RO, Aditya A (2023) Calculation array solar panel capacity of 50 kWP Pamulang University South Tangerang. *Triyanto* 10: 193–198. https://doi.org/10.33387/protk.v10i3.5795
26. Saidur R, Abdelaziz EA, Demirbas A, et al. (2011) A review on biomass as a fuel for boilers. *Renewable Sustainable Energy Rev* 15: 2262–2289. https://doi.org/10.1016/j.rser.2011.02.015
27. Zhao N, Li BW, Ahmad R, et al. (2021) Dynamic relationships between real-time fuel moisture content and combustion-emission-performance characteristics of wood pellets in a top-lit updraft cookstove. *Case Stud Thermal Eng* 28: 101484. https://doi.org/10.1016/j.csite.2021.101484
28. Demirbas A (2007) Effects of moisture and hydrogen content on the heating value of fuels. *Energy Sources, Part A* 29: 649–655. https://doi.org/10.1080/009083190957801
29. Ujam AJ, Eboh F (2012) Thermal analysis of a small-scale municipal solid waste-fired steam generator: Case study of Enugu state, Nigeria. *J Energy Technol Policy* 2: 2327. Available from: https://www.iiste.org/Journals/index.php/JETP/article/view/2327/2327.
30. Obenberger, Thek IG (2010) The pellet handbook. IEA bioenergy. Earthscan LLC, Washington, DC.
31. Clement AK, Iyiola OO, Omojola A, et al. (2019) Experimental investigation and thermal analysis of solar air heaters having rectangular rib roughness on the absorber plate. *Case Stud Therm Eng* 14: 100442. https://doi.org/10.1016/j.csite.2019.100442
32. Sukhatme SP, Nayak JK (2018) Solar energy. Fourth Edition. Tata McGraHill Publishing Company, New Delhi.
33. Symons JG (1984) Calculation of the transmittance-absorptance product for flat-plate collectors with convection suppression devices. *Sol Energy* 33: 637–640. https://doi.org/10.1016/0038-092X(84)90023-9
34. Climate classification. Available from: https://en.wikipedia.org/wiki/Köppen_climate_classification.
35. Boumanchar I, Chhiti Y, M'hamdi Alaoui FE (2019) Municipal solid waste higher heating value prediction from ultimate analysis using multiple regression and genetic programming techniques. *Waste Manage Res* 37: 578–589. https://doi.org/10.1177/0734242X18816797

36. Phillips OA, Jehad S (2016) Feasibility of municipal solid waste (MSW) as energy sources for Saudi Arabia's future Reverse osmosis (RO) desalination plants. *Polish J Chem Technol* 18: 82–89. https://sciendo.com/article/10.1515/pjct-2016-0075
37. Hegde VN, Hosur VS, Rathod SK, et al. (2015) Design, fabrication and performance evaluation of solar dryer for banana. *Energy Sustain Soc* 5: 15–52. https://doi.org/10.1186/s13705-015-0052-x
38. Jangde K, Singh A, Arjunan TV (2022) Efficient solar drying techniques: A review. *Environ Sci Pollut Res* 29: 50970–50983. https://doi.org/10.1007/s11356-021-15792-4
39. Boonthum E, Sirichana S, Namkhet A (2024) Comparative study on performance of passive and active solar dryer. *Key Eng Mater* 978: 97–103. https://doi.org/10.4028/p-2GFc9W
40. Okta Arifianti QAM, Abidin MR, Nugrahani EF, et al. (2018) Experimental investigation of a solar greenhouse dryer using fiber plastic cover to reduce the moisture content of refuse derived fuel in an Indonesian cement industry. *2018 International Conference and Utility Exhibition on Green Energy for Sustainable Development (ICUE),* Phuket, Thailand, 2018, 1–5. https://doi.org/10.23919/ICUE-GESD.2018.8635723

AIMS Press